

# Pterin pigment granules are responsible for both broadband light scattering and wavelength selective absorption in the wing scales of pierid butterflies

Nathan I. Morehouse<sup>1,\*</sup>, Peter Vukusic<sup>2</sup> and Ron Rutowski<sup>1</sup>

<sup>1</sup>*School of Life Sciences, Arizona State University, Tempe, AZ 85287, USA*

<sup>2</sup>*School of Physics, University of Exeter, Exeter EX4 4QL, UK*

A small but growing literature indicates that many animal colours are produced by combinations of structural and pigmentary mechanisms. We investigated one such complex colour phenotype: the highly chromatic wing colours of pierid butterflies including oranges, yellows and patterns which appear white to the human eye, but strongly absorb the ultraviolet (UV) wavelengths visible to butterflies. Pierids produce these bright colours using wing scales that contain collections of minute granules. However, to date, no work has directly characterized the molecular composition or optical properties of these granules. We present results that indicate these granules contain pterin pigments. We also find that pterin granules increase light reflection from single wing scales, such that wing scales containing denser granule arrays reflect more light than those with less dense granule collections. As male wing scales contain more pterin granules than those of females, the sexual dichromatism found in many pierid species can be explained by differences in wing scale pterin deposition. Additionally, the colour pattern elements produced by these pterins are known to be important during mating interactions in a number of pierid species. Therefore, we discuss the potential relevance of our results within the framework of sexual selection and colour signal evolution.

**Keywords:** animal coloration; nano-optics; trait evolution; pierid butterflies; structural colour; pterin pigments

## 1. INTRODUCTION

Bright animal colours are perhaps some of the most intriguing and poorly understood natural phenomena, and continue to preoccupy scientists working at all levels of scientific inquiry. Recent advances in fields as disparate as optical physics, pigment biochemistry, behavioural ecology and developmental biology suggest that understanding the physical makeup of animal colorants and colour patterns has the potential to inform a host of interesting questions regarding the development and evolution of bright colours (e.g. Bradbury & Vehrencamp 1998; Grether *et al.* 2004; Hill & McGraw 2006). For example, recent work on carotenoid biochemistry and metabolism has revealed the importance of dietary dependence and physiological trade-offs in determining the role of these pigments as sources of information in sexually selected vertebrate colour displays (Grether *et al.* 1999, 2005; Hill 1999; McGraw & Hill 2000). Likewise, analyses of other pigment-based and structurally generated colour elements have reinforced the idea that the identity of animal colorants has strong implications for their utility as signals in behavioural interactions (Badyaev & Hill 2000; Jawor & Breitwisch 2003; Freitak *et al.* 2005; Hill *et al.* 2005).

Research on the mechanisms that animals employ in producing their bright colours has demonstrated that single colours often arise from combinations of optical phenomena (Grether *et al.* 2004; Vukusic *et al.* 2004; Rutowski *et al.*

2005; Shawkey & Hill 2005; Yoshioka & Kinoshita 2006). This small but growing body of work paints a more complex picture of animal colour production than has been considered previously, and it is likely to strongly influence our appreciation of the behavioural and ecological significance of bright animal colours. In particular, animal colours that have traditionally been considered to be pigment-based may need to be re-evaluated if previously unconsidered structural phenomena contribute significantly to extant variation in these colours (or, in the case of ‘structural colours’, vice versa). At a very basic level, what these more rigorous evaluations of animal colours suggest is that measuring just pigment concentrations or only the nano-spatial periodicity of optical structures may at times be insufficient to describe the relevant sources of variation in a given colour trait.

This is particularly true for butterfly colours, where some of nature’s most complex and diverse colour-producing structures have been described (Ghiradella 1991; Vukusic *et al.* 2000; Kemp 2002). Previous work on ‘structural colours’ in butterflies has relied heavily on inferences from electron microscopy (e.g. Ghiradella 1991; Vukusic *et al.* 2000, 2001a). However, while these techniques provide fine-scale spatial information, they often cannot identify the molecular makeup of the imaged structures, and therefore leave us without an understanding of the spatial arrangement or potential participation of pigments in these colours. On the other hand, analyses of butterfly colours thought to arise predominantly from pigmentary light absorption have relied

\* Author for correspondence (nmorehouse@asu.edu).

instead on pigment extraction and quantification from whole wing regions, resulting in extremely coarse estimates of the spatial distribution of pigment deposits.

Here, we present results from a series of analyses which allow us to identify both the spatial arrangement and optical consequences of pterin pigment deposits in the wing scales of pierid butterflies. Previous research has suggested that pterins are deposited in nanoscale granules suspended between the upper and the lower lamina of pierid wing scales (Yagi 1954; Kolyer & Reimschuessel 1970; Waku & Kitagawa 1986; Rutowski *et al.* 2005). In addition, results from work by Stavenga *et al.* (2004) hint that these granules may be involved in augmenting broadband light scattering from wing surfaces. However, to date no work has directly tested either possibility. Therefore, we sought to characterize both the molecular makeup and optical properties of these scale granules, with the hope that the findings would better inform our understanding of bright pierid wing colours, and the morphological constituents responsible for inter- and intrasexual colour variation found across the clade (Bowden 1977; Meyer-Rochow & Järvillehto 1997; Obara & Majerus 2000).

## 2. MATERIAL AND METHODS

### (a) *Animals*

Confocal and SEM analyses were conducted for *Pontia protodice* and *Colias eurytheme*. Spectral measurements of colour patterns on intact and pterin-extracted wings (see §3) and optical characterization of single wing scales were performed on samples from *P. protodice*. *Colias eurytheme* individuals were collected during 2004 and 2005 from field populations surrounding Phoenix, Arizona. *Pontia protodice* individuals were laboratory-reared in 2005 on *Sisymbrium irio* under a steady temperature (approx. 25°C) and humidity regime, and a 14L : 10D cycle. Adults were freeze-killed upon collection and their wings or wing scales removed for analyses.

### (b) *Spectral analysis of pterin contribution to wing coloration*

To determine the spectral contributions of pterin pigments to wing coloration, reflectance spectra were collected from the dorsal surface of the  $Cu_1$ – $Cu_2$  cell of forewing samples from *P. protodice*, a wing region that appears white to the human eye, but is strongly UV absorbing owing to the presence of pterin pigments. Spectral collection methods followed those described in Rutowski *et al.* (2005). Briefly, forewings were mounted on black cardstock and spectra collected using a spectrophotometer (model USB2000, Ocean Optics, Inc.) whose collimated collector was positioned at a 45° elevation relative to the plane of the wing. The samples were illuminated using a pulsed xenon light source (model PX-2, Ocean Optics, Inc.) with its light path oriented normal to the wing surface. All spectra were normalized relative to a white standard created by coating a glass microscope slide with MgO. After spectra were collected from intact wings, the wings were immersed in 0.1 M  $NH_4OH$ , a technique that extracts pterin granules from the wings while leaving other scale structures intact (Rutowski *et al.* 2005). Spectra were collected from the resulting pterin-less wing samples as described above.

### (c) *Determination of spatial arrangement of pterin pigment deposits*

Wing samples, either intact or with pterins extracted, were removed from the dorsal  $Cu_1$ – $Cu_2$  forewing cell and mounted on standard SEM stubs with the dorsal surface facing upwards, using conductive carbon adhesive. Samples were sputter-coated with approximately 10 nm of gold, and imaged at an acceleration voltage of 15 kV with a scanning electron microscope (Leica-Cambridge Stereoscan 360 FE, Leica-Cambridge Ltd.). The size of scale features, including scale granules, was then measured from digital images using IMAGEJ software (NIH freeware, <http://rsb.info.nih.gov/ij/>).

Confocal microscopy uses light emitted from fluorescent molecules to generate images of microscopic structures. As pterin pigments fluoresce when stimulated with short-wavelength light (Fox 1976), we were able to image directly the spatial location of pterin deposits within the wing scales in the following way. Scales from the areas neighbouring those imaged in SEM analyses, including those with pterins removed, were mounted on standard microscope slides using high-viscosity immersion oil and glass cover slips. These samples were then imaged using a laser scanning confocal microscope (model TCS SP2, Leica Microsystems Inc.). All samples were stimulated at an excitation wavelength of 488 nm, and emitted light was collected from 500 nm to 700 nm. Using this wavelength range, two-dimensional images were collected at regular intervals along the vertical focal plane, enabling three-dimensional characterization of fluorescent structures within the wing scales.

To verify that the emitted light used to create the images was indeed derived from pterin pigments and not from other light-emitting compounds, emission spectra were collected from fluorescent wing scale structures at 5 nm intervals from 500 nm to 700 nm using an excitation wavelength of 458 nm. These spectra were then compared to emitted light spectra collected from purified pterin samples, including sepiapterin, xanthopterin, isoxanthopterin, leucopterin (Sigma Chemical Co. and Schirk Labs) and erythropterin (obtained from W. Pfeleiderer), which were prepared and imaged in the same way as wing samples. These purified pterins represent all pterins known to occur in the wings of *C. eurytheme* (Watt 1964) and *P. protodice* (N. I. Morehouse 2006, unpublished data).

### (d) *Optical characterization of single wing scales*

We characterized the optical properties of individual *P. protodice* wing scales using methods modified from Vukusic *et al.* (1999). Single scales were removed from the  $Cu_1$ – $Cu_2$  cell of the dorsal forewing surface and mounted by their basal end to the tip of a ground needle using two-compound epoxy and a micromanipulator (figure 1a). Scale position on the needle tip was verified using an optical microscope. The needle and attached scale were then mounted at the centre of an Euler cradle, which was coincident with the path of a focused laser beam. Using an optical microscope, an achromatic lens and micromanipulators associated with the Euler cradle, we guaranteed that the laser beam was focused normal to the dorsal surface of the wing scale and positioned centrally within the distal third of the scale (shaded region in figure 1a). This resulted in a diffraction-limited minimum beam waist of approximately 30  $\mu$ m in diameter focused on the wing scale surface. All measurements were conducted sequentially using two HeNe lasers with wavelengths of 543 nm and 633 nm. Preliminary measurements indicated

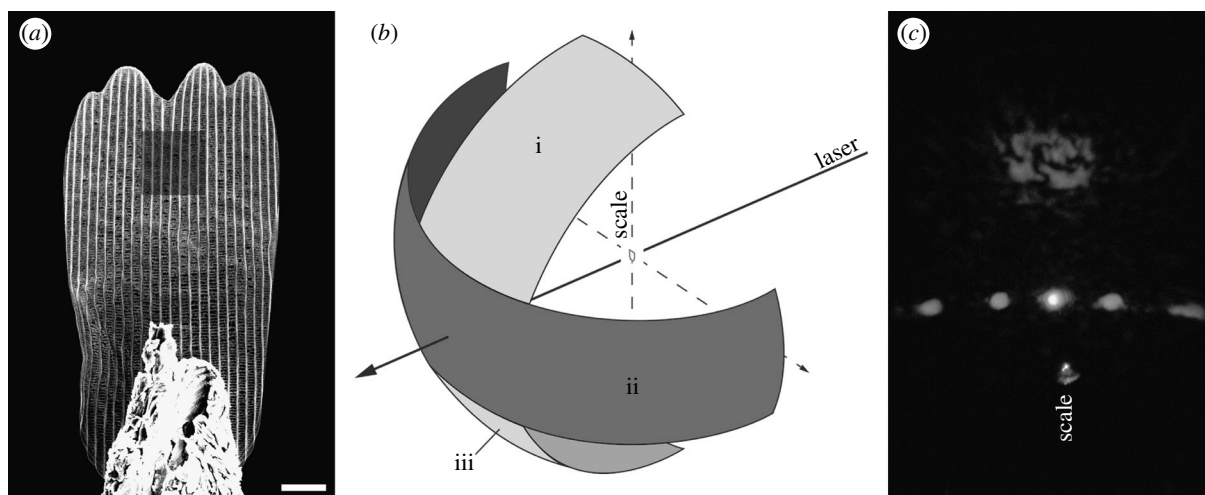


Figure 1. Illustrations of experimental protocols for measurement of transmittance through single scales. (a) SEM image of single scale mounted to the tip of a needle. Shaded square represents the location where laser beams were focused during transmission and absorption measurements as well as where SEM data on granule array density were collected. Scale bar, 10  $\mu\text{m}$ . (b) Diagram of light collected during transmission measurements. Light was collected in a horizontal band  $40^\circ$  wide and  $180^\circ$  long (ii) and separately in a vertical band  $40^\circ$  wide and  $70^\circ$  long (i). Experimental setup prevented the direct collection of the lower half of the vertical band (iii), so this was estimated by assuming symmetry of transmitted light and using values from (i). Total transmittance was estimated by summing (i), (ii) and (iii). Diagram not to scale. (c) Example of the pattern of light transmitted through a scale, showing concentration of light in two diffraction orders falling within single vertical and horizontal bands that coincide with areas where transmitted light was collected.

that reflection from the scale surface was too diffuse to be directly quantified with sufficient accuracy. Therefore, we chose to estimate reflectance from measures of scale transmittance and absorption as follows.

#### (i) Scale transmittance

Measurements of scale transmittance were obtained using a collector mounted to a computer-controlled motorized table whose centre corresponded to the centre of the Euler cradle. This allowed for light collection to occur every  $0.1^\circ$  along the  $180^\circ$  horizontal perimeter behind the mounted scale (figure 1b). Transmitted light was focused on to the collector using a lens with a collection angle of  $40^\circ$ , thus enabling us to collect vertically spread transmitted light in a  $40^\circ$  swath along the horizontal axis. Horizontal resolution of collected light was improved by placing a vertical slit in front of the collector lens, thus limiting collection of horizontally spread light to approximately  $4^\circ$ .

Owing to diffraction caused by the periodicity of longitudinal scale ridges and horizontal scale cross ribs, light transmitted through the wing scales was concentrated in single, narrow vertical and horizontal bands (figure 1c). Therefore, we were able to collect virtually all transmitted light using two sets of measurements per scale per laser wavelength. The first was an  $180^\circ$  band along the horizon behind the scale with the scale mounted vertically (figure 1b(ii)). This allowed us to collect all light diffracted along the horizontal transmission band. We then rotated the scale  $90^\circ$  counterclockwise within the Euler cradle, ensuring that the scale remained at the centre of the cradle and that the laser beam was still focused at the same point within the distal third of the scale. In this orientation, light was collected from  $110^\circ$  to  $180^\circ$  (with  $90^\circ$  corresponding to directly behind the scale, figure 1b(i)). This shorter angular measurement span along the vertical transmission band was due to obstruction of transmitted light from  $0^\circ$  to  $70^\circ$  by the mounting apparatus holding the needle and scale, and also due to the fact that light from  $70^\circ$  to  $110^\circ$  in the vertical band corresponded to light

already collected during horizontal band measurements. In addition, for each measurement described above, a corresponding value of total photon flux was derived by collecting light from  $80^\circ$  to  $110^\circ$  without the scale in place. Spread of unobstructed laser light never exceeded this range.

Transmittance for each measurement was then calculated from the integrated transmission and total photon flux measurements. As collection of light from the vertical transmission band was limited to the upper half of the band, values derived from these measurements were doubled by assuming symmetry of transmission (figure 1b(iii)). Total transmittance for each scale was then calculated by summing transmittance values from vertical and horizontal transmission bands. We note that while we collected the vast majority of light transmitted through the wing scales, light was not collected from a small proportion of the hemisphere behind the mounted scales (figure 1b). Therefore, it is possible that our measurements of transmittance slightly underestimate actual total transmittance, resulting in inflated values for total reflectance. However, we would expect this source of error to be negligible and to apply equally to transmittance values from all the scales measured, thus leaving the qualitative conclusions of our results intact.

We derived the total transmittance values for single scales from 15 *P. protodice* individuals (5 males, 10 females), chosen to represent the naturally occurring range of granule array densities. In addition, scales from a subset of these same individuals were subjected to pterin extraction as described above, and total transmittance values derived from these pterin-less (and granule-less) scales (2 males, 3 females, total  $n=5$ ).

#### (ii) Scale absorption

We expected light absorption to be negligible at the laser wavelengths used (543 nm and 633 nm) because pterin pigments found in *P. protodice* wings do not exhibit any appreciable absorption at either wavelength (Blakley 1969; N. I. Morehouse 2006, unpublished data). Therefore, we



chose to derive values for scale absorption from a small subset of scales (2 females, 2 males and 2 extracted scales, total  $n=6$ ).

Methods for measuring scale absorption were similar to those for scale transmittance. All measurements were taken on scales immersed in an index-matching fluid (cuticle refractive index =  $1.56 \pm 0.05$ , Vukusic *et al.* 1999; immersion fluid refractive index =  $1.52 \pm 0.01$ , Cargille Laboratories Inc.), under the assumption that such treatment would eliminate light reflection by the scale (but see below). In the absence of light reflection from the scale, absorption can be calculated as the percentage of total photon flux that is transmitted through the immersed scale subtracted from 100%. Therefore, we measured light transmittance through single immersed scales and the immersion fluid with the scales removed. Both measurements were taken only in the horizontal plane from  $80^\circ$  to  $100^\circ$ , as diffraction of light by the scale and immersion fluid was negligible. Scale absorption was then calculated by comparing integrated measurements of scale transmittance and total photon flux.

We acknowledge that the index-matching fluid used may not have matched the refractive index of the pterin deposits in the wing scales measured. These deposits are likely to have a higher refractive index than that of cuticle and the index-matching fluid (the refractive index of guanine, a pterin precursor, is 1.83, Herring 1994). Therefore, our index-matching protocol should reduce but not eliminate light reflection by the scale (Stavenga *et al.* 2006). Such a complicating factor could lead to erroneous inflation of measurements of scale absorbance. However, our empirical results (see below) suggest that this source of error is too small for us to detect and therefore of limited concern in this study.

### (iii) SEM measurements of granule density

The same scales measured for total transmittance were then subjected to SEM imaging to obtain measurements of granule array density, or in the case of the extracted scales, to verify that extraction had removed most or all of the granules from the scales. While still attached to needle tips, these scales were mounted on standard SEM stubs, sputter coated with approximately 10 nm chromium dioxide and imaged using a scanning electron microscope (FEI Novalab 600 Dual-beam, FEI Co.) at an acceleration voltage of 15 kV. Images were then captured from the same regions where lasers were focused for optical measurements (shaded region in figure 1a). From these images, the number of granules within a  $25 \mu\text{m}^2$  area was counted and used as a measure of granule array density. Using linear regression, the results from unextracted scales were then compared to corresponding values of total scale reflectance calculated from transmission and absorption results.

### (e) Statistics

All statistical analyses detailed below were performed using SYSTAT v. 10 (SYSTAT Software, Inc.). Normality and equal variance of data were verified prior to running statistical tests. We report central tendency as mean  $\pm$  standard error.

## 3. RESULTS

### (a) Spectral analysis of pterin contribution to wing coloration

Spectral measurements from untreated dorsal forewing surfaces of three male and three female *P. protodice* reveal a

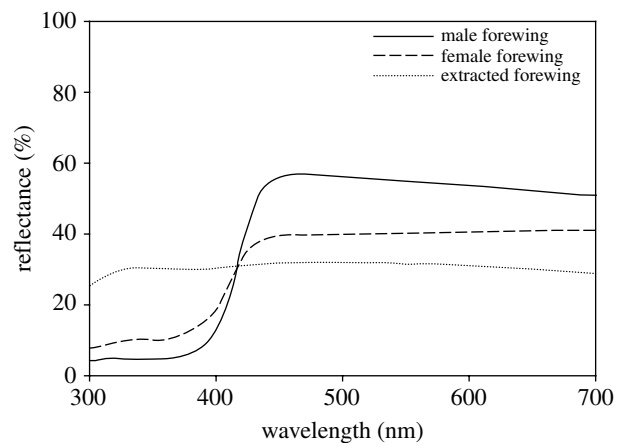


Figure 2. Reflectance spectra measured from dorsal forewing regions of male ( $n=3$ ) and female ( $n=3$ ) *P. protodice* individuals, both before and after pterin extraction. As spectra from extracted wings did not differ significantly between the sexes, the extracted spectral curve is an average of measurements from both sexes.

clear pattern of sexual dichromatism (see figure 2). When compared with female conspecifics, the 'white' regions of male wings exhibit higher reflectance of long-wavelength light (450–700 nm, male =  $54.16 \pm 3.04\%$ , female =  $40.32 \pm 4.52\%$ ; Student's  $t$ -test:  $t=2.541$ , d.f. = 4,  $p=0.032$ ) and lower reflectance of short-wavelength light (300–375 nm, male =  $4.78 \pm 0.98\%$ , female =  $9.70 \pm 1.24\%$ ; Student's  $t$ -test:  $t=3.117$ , d.f. = 4,  $p=0.018$ ). Removal of pterins from the forewings resulted in two main effects on dorsal coloration (figure 2). First, reflectance of short-wavelength light (300–375 nm) increased in extracted wings (unextracted wings =  $7.23 \pm 1.30\%$ , extracted wings =  $29.45 \pm 1.87\%$ ; paired  $t$ -test:  $t=9.501$ , d.f. = 5,  $p<0.0001$ ), as expected from the loss of short-wavelength absorption associated with pterins known to be found in both species (Watt 1964; N. I. Morehouse 2006, unpublished data). Additionally, pterin extraction reduced the reflectance of long-wavelength light (unextracted wings =  $47.24 \pm 3.94\%$ , extracted wings =  $30.99 \pm 2.44\%$ ; paired  $t$ -test,  $t=5.433$ , d.f. = 5,  $p=0.003$ ), suggesting a loss of structural scattering associated with pterin removal.

### (b) Determination of spatial arrangement of pterin pigment deposits

SEM analyses revealed arrays of oblong granules suspended between the upper and the lower lamina of the wing scales in both species, with granule length and width averaging *ca* 300 nm and 130 nm, respectively for *P. protodice* and *ca* 450 nm and 170 nm, respectively for *C. eurytheme*. Male *P. protodice* had denser granule arrays than did females of the same species (number of granules per  $25 \mu\text{m}^2$ , male =  $591.00 \pm 42.37$ , female =  $443.21 \pm 49.14$ , Student's  $t$ -test:  $t=2.278$ , d.f. = 30,  $p=0.030$ , figure 3a,c), with intermediate granule array densities found in both sexes of *C. eurytheme* (figure 3e). Pterin-extracted wing samples from all species confirmed that this procedure removed granules while leaving other scale features intact.

Confocal images revealed collections of fluorescent compounds that coincided in shape, location and spatial density to the granules seen in SEM images (figure 3b,d,f).

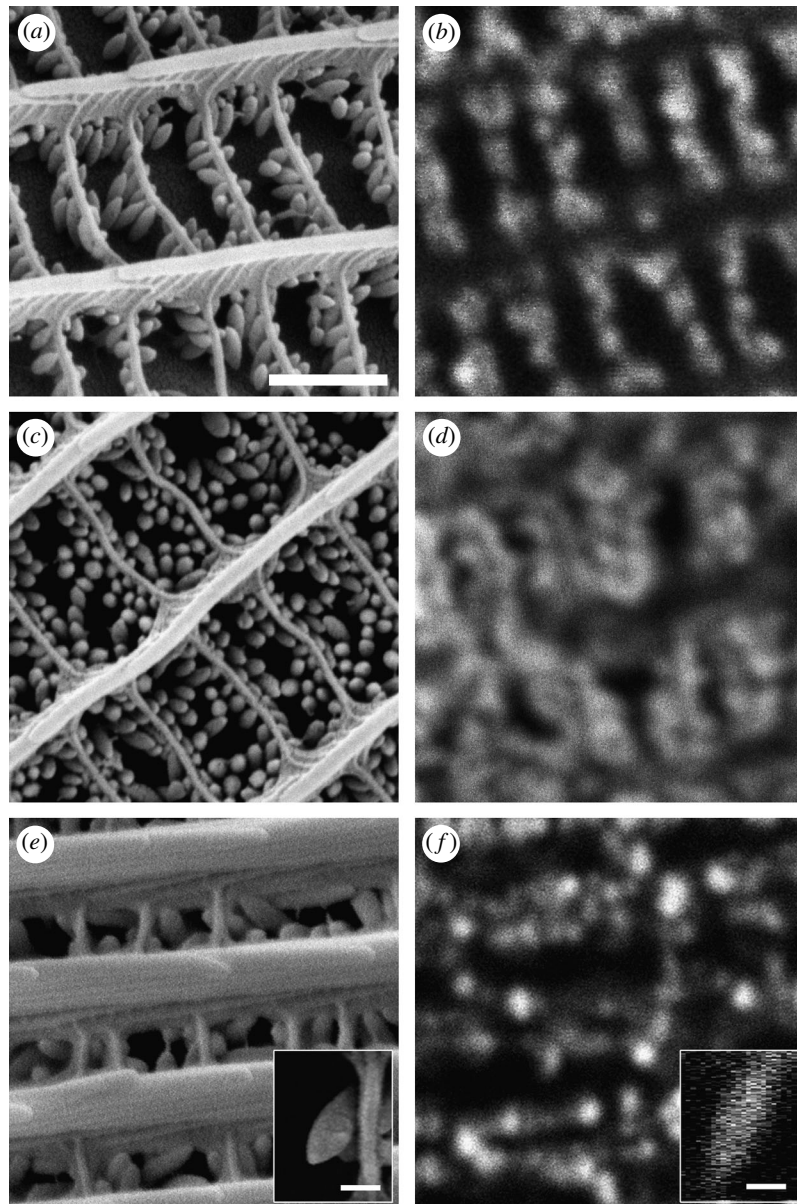


Figure 3. (a,c,e) SEM and (b,d,f) confocal images of dorsal forewing scales from *Pontia protodice* female (a,b) and male (c,d) and *Colias eurytheme* male (e,f). In all the cases, images were taken from similar but not identical scales from each species. Insets (e,f) are side profiles of single scale granules from a male *C. eurytheme*. The confocal inset image was generated via digital reconstruction from a stack of confocal images taken at known intervals along the vertical focal plane. All the images correspond to each other in scale (scale bar, 1  $\mu\text{m}$ ), with the exception of insets (scale bars, 250 nm).

In addition, granule (and pterin) extraction removed all fluorescence from wing samples. Emission spectra collected from non-extracted wing samples corresponded well with those derived from purified pterin standards. However, in no species did wing emission spectra exactly match emission spectra from a single purified pterin. Instead, emission spectra from wing samples were always intermediate between emission spectra from several purified pterins, which suggests that pterins are deposited as mixtures within wing scales.

#### (c) Optical characterization of single wing scales

Values for scale absorption from all the scales measured did not significantly differ from zero for the 543 nm laser (mean absorption =  $-0.51\%$ ; 95% confidence interval:  $-2.68$  to  $1.66\%$ ) and were negative for the 633 nm laser (mean absorption =  $-1.33\%$ ; 95% confidence limits:  $-2.00$  to  $-0.66\%$ ). However, absorption results from the two laser

wavelengths did not significantly differ (paired *t*-test:  $t=0.931$ , d.f. = 10,  $p=0.374$ ). We therefore concluded that scale absorption at 543 nm and 633 nm was negligible, and we chose to calculate scale reflectance at these wavelengths using scale transmittance subtracted from 100%.

Using the resulting reflectance values, we first evaluated the effect of pterin granule removal on the reflection of light off single scales. We found that removal of pterin granules significantly reduced the reflectance of light off single scales (unextracted =  $62.05 \pm 2.55\%$ , extracted =  $42.70 \pm 3.33\%$ ,  $F=32.27$ , d.f. = 1,  $p<0.0001$ ). In addition, reflectance values for the 633 nm laser were lower than those from the 543 nm laser for both extracted and unextracted scales ( $F=10.435$ , d.f. = 1,  $p=0.007$ ), consistent with reduced reflectance at higher wavelengths found in spectra from male and extracted wing regions (see figure 2), but not female wing spectra.

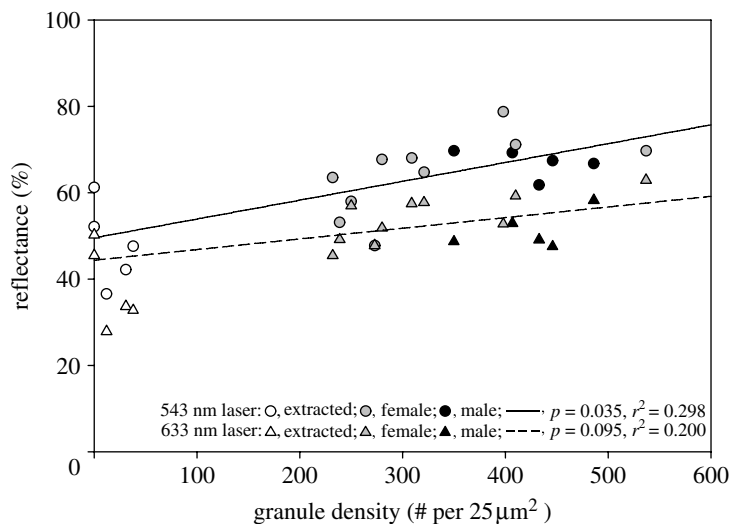


Figure 4. Plot of granule array density versus scale reflectance. Measurements for both variables were conducted on the same regions of the same scales. Regression lines indicate a positive correlation between granule array density and scale reflectance within the natural range of variation, which is significant for measurements using the 543 nm laser and consistent, but not significant, for measurements at 633 nm. Values from extracted scales are added for illustration, but were not included in regression calculations. However, note the close correspondence between actual values from extracted scales (scales with artificially lowered granule densities) and predicted values from regression equations derived solely from unextracted scale values. Also, note that most values for intact female scales fall below those for males, presenting a possible mechanism for the sexual dichromatism found in this species (see figure 2).

We then explored the possibility that the density of granules deposited within wing scales *per se* might influence the amount of light that scales reflect. Unextracted scales with recorded reflectance values (5 males, 10 females,  $n = 15$ ) were measured for the density of their granule arrays using SEM as described above. These samples exhibited a range of granule array densities representative of naturally occurring phenotypic variation (N. I. Morehouse 2006, unpublished data). We regressed granule array density values against total scale reflectance measurements separately for each laser wavelength (figure 4). We found that within the natural phenotypic range of variation, granule array density was positively correlated with total scale reflectance. This result was significant for measurements at 543 nm ( $r^2 = 0.298$ ,  $p = 0.035$ ), with a consistent but not significant trend for measurements at 633 nm ( $r^2 = 0.200$ ,  $p = 0.095$ ). We expect that results would have been statistically significant for measurements at 633 nm if sample sizes had been larger. As with comparison of extracted and unextracted scales, measurement values derived at 633 nm were uniformly lower than those from the 543 nm laser. In addition, when placed along the regression lines from this analysis, extracted scales correspond well with predicted values for scales with granule array densities approaching zero (see figure 4), lending further support to the idea that granule array density *per se* influences the amount of light scattered off of single scales.

#### 4. DISCUSSION

Our results provide direct empirical evidence that pierid butterflies deposit pterin pigments within the nanoscale granules in their wing scales, and that these granules act to increase the reflection of light wavelengths they do not absorb. The key support presented for this conclusion can be summarized as follows. Pierid wing scales contain arrays of oblong, nanoscale granules, which when

stimulated with short-wavelength light, emit longer wavelength light consistent in spectral shape to the pterin pigments known to occur in the wings. Removal of these granules via extraction eliminates scale fluorescence and significantly reduces the amount of long-wavelength light reflected from single scales. In addition, the density of granule arrays within individual wing scales influences the amount of incident long-wavelength light reflected from the surface of a given scale, such that scales with denser collections of granules reflect more light than do scales with more sparsely populated arrays. This relationship is consistent across the naturally occurring range of granule array densities for *P. protodice*, and we expect the same relationship to hold for other pierid butterflies.

These results have several significant implications. First, to our knowledge, this represents a unique case where collections of pigment molecules simultaneously absorb one wavelength range while augmenting the reflection of another. As such, semi-ordered deposits of pterin pigments produce the highly chromatic colours found in pierid butterflies by a combination of pigmentary absorption and structural reflection (as suggested by Rutowski *et al.* 2005). While our results present the first description of this type, we expect that complex colour phenotypes involving simultaneous 'structural' and 'pigmentary' roles for pigment deposits are not uncommon. For example, melanin is known to participate in the thin-film systems responsible for the brilliant gorgets of hummingbirds (Greenewalt *et al.* 1960) and the wing colours of papilionid butterflies (Vukusic *et al.* 2001b). In these systems, melanin deposits are likely to influence both the refractive index of reflecting nanostructures, and the spectral purity of the colour patterns by reducing the amount of extraneous light that is backscattered from the integument (e.g. Yoshioka & Kinoshita 2006).

Even in cases where pigment molecules do not directly contribute to both structural and pigmentary phenomena, a deeper understanding of phenotypic determinants of



coloured structures can be gained by looking at the arrangement of reflecting nanostructures and coincident pigment deposits. For example, Prum & Torres (2003) reported unique colour effects in avian skin coloration owing to the combined contributions of carotenoids and collagen nanostructures, and similar interactions have been demonstrated for avian plumage (Shawkey & Hill 2005). Vukusic *et al.* (2004) described a system where a combination of melanin deposits and light-scattering wing scale features results in increases in light absorption on the wings of an African swallowtail, *Papilio ulysses*. Rutowski *et al.* (2005) recently reported the central role that pterin pigments play in showcasing structurally generated ultraviolet reflection in male *C. eurytheme*. These examples highlight an important point about animal coloration that has only recently begun to be explored in earnest, namely that many if not most animal colours are produced by complex interplays between pigment molecules and integumentary structures.

While the more rigorous evaluations motivated by this perspective will help us to better understand *how* animals produce their often vivid colours, they also promise to inform questions about *why* animals are so brightly coloured. Animal colours that are generated from the combined effects of several optical phenomena hold the potential to communicate multiple pieces of information about their bearers to conspecifics (Grether *et al.* 2004), especially if different components of a given colour trait impose distinct costs on an individual. This may be particularly relevant in the context of sexual selection during intra- or intersexual competition for mates, and it is worth noting that all the examples cited above involve colours used in sexually dimorphic displays.

Such ideas are likely to be useful for understanding the evolution of the pterin-based colour phenotypes investigated here. As spectral data from *P. protodice* attest (figure 2), males of this species have more highly chromatic, pterin-based wing colours than do their female conspecifics, a pattern which is common across the Pieridae (Makino *et al.* 1952; Obara & Hidaka 1968; Descimon 1975; Bowden 1977; Meyer-Rochow & Järvillehto 1997; Obara & Majerus 2000). Additionally, previous work has shown that pterin-based sexual dichromatism is important to mating decisions by members of both sexes in *P. protodice* (Rutowski 1981). Similar results have been found in other pierid species (e.g. Obara 1970). We now know that the common mechanism underlying these sex-linked differences in wing coloration is differential deposition of pterin granules, such that males deposit higher levels of pterins in their wings resulting in denser granule arrays (consistent with previous findings, e.g. Makino *et al.* 1952; Watt & Bowden 1966; Hidaka & Okada 1970). Our results also indicate that intrasexual colour variation is determined by the amount of pterins individuals deposit within their wing scales. However, little is known about the costs imposed by dense pterin granule arrays, and therefore whether pterin-based colour variation might encode information about an individual's health or quality. Work in our laboratory is ongoing to explore potential nutritional and energetic costs imposed by the production of pterin granule arrays as well as their role in mediating behavioural interactions.

The results of our study point to specific avenues for future research on pierid wing coloration and offer a more

complete understanding of the basic constituents of these colour phenotypes. However, we suggest that the ideas and techniques described here could be applied to the larger collection of animal colours and colour patterns. Paying close attention to the optical mechanisms and the physical components of animal colours from a variety of species is likely to produce both surprising results and valuable insights into the production and evolution of bright animal colours.

We thank J. Macedonia for help with spectral analyses, the insight to use confocal microscopy and many stimulating conversations on pierid wing coloration; Kevin McGraw and W. Pfleiderer for providing purified erythropterin; D. Stavenga for helpful conversations and comments; C. Kazilek and P. Baluch for help with confocal work; W. Sharp for SEM assistance; and Joe Noyes for help with optical measurements. The work presented here was supported by the School of Life Sciences at Arizona State University, NSF grant no. IBN 0316120 to RLR, and a Grant-In-Aid of Research from Sigma Xi, The Scientific Research Society to NIM.

## REFERENCES

- Badyaev, A. V. & Hill, G. E. 2000 Evolution of sexual dichromatism: contribution of carotenoid- versus melanin-based coloration. *Biol. J. Linn. Soc.* **69**, 152–172. (doi:10.1006/bjll.1999.0350)
- Blakley, R. L. 1969 *The biochemistry of folic acid and related pteridines*. *Frontiers of biology*. Amsterdam, The Netherlands: North Holland Publishing Company.
- Bowden, S. R. 1977 *Pieris* (Lepidoptera, Pieridae)—the ultraviolet image. *Proc. Brit. Ent. Nat. Hist. Soc.* **10**, 16–22.
- Bradbury, J. W. & Vehrencamp, S. L. 1998 *Principles of animal communication*. Sunderland, MA: Sinauer Associates, Inc.
- Descimon, H. 1975 Biology of pigmentation in pieridae butterflies. In *Chemistry and biology of pteridines. Proceedings of the 5th International symposium* (ed. W. Pfleiderer), pp. 805–840. New York, NY: Walter De Gruyter.
- Fox, D. L. 1976 *Animal biochromes and structural colors: physical, chemical, distributional and physiological features of colored bodies in the animal world*. Berkeley, CA: University of California Press.
- Freitak, D., Vanatoa, A., Ots, I. & Rantala, M. J. 2005 Formation of melanin-based wing patterns is influenced by condition and immune challenge in *Pieris brassicae*. *Entomol. Exp. Appl.* **116**, 237–243. (doi:10.1111/j.1570-7458.2005.00330.x)
- Ghiradella, H. 1991 Light and color on the wing: structural colors in butterflies and moths. *Appl. Opt.* **30**, 3492–3500.
- Greenewalt, C. H., Brandt, W. & Friel, D. D. 1960 Iridescent colors of hummingbird feathers. *J. Opt. Soc. Am.* **50**, 1005–1013.
- Grether, G. F., Hudon, J. & Millie, D. F. 1999 Carotenoid limitation of sexual coloration along an environmental gradient in guppies. *Proc. R. Soc. B* **266**, 1317–1322. (doi:10.1098/rspb.1999.0781)
- Grether, G. F., Kolluru, G. R. & Nersissian, K. 2004 Individual colour patches as multicomponent signals. *Biol. Rev.* **79**, 583–610. (doi:10.1017/S1464793103006390)
- Grether, G. F., Kolluru, G. R., Rodd, F. H., de la Cerda, J. & Shimazaki, K. 2005 Carotenoid availability affects the development of a colour-based mate preference and the sensory bias to which it is genetically linked. *Proc. R. Soc. B* **272**, 2181–2188. (doi:10.1098/rspb.2005.3197)
- Herring, P. J. 1994 Reflective systems in aquatic animals. *Comp. Biochem. Phys. A* **109**, 513–546. (doi:10.1016/0300-9629(94)90192-9)

- Hidaka, T. & Okada, M. 1970 Sexual differences in wing scales of the white cabbage butterfly, *Pieris rapae crucivora*, as observed under a scanning electron microscope. *Zool. Mag.* **79**, 181–184.
- Hill, G. E. 1999 Is there an immunological cost to carotenoid-based ornamental coloration? *Am. Nat.* **154**, 589–595. (doi:10.1086/303264)
- Hill, G. E. & McGraw, K. J. (eds) 2006 *Bird coloration: mechanisms and measurements*, vol. 1. Cambridge, MA: Harvard University Press.
- Hill, G. E., Doucet, S. M. & Buchholz, R. 2005 The effect of coccidial infection on iridescent plumage coloration in wild turkeys. *Anim. Behav.* **69**, 387–394. (doi:10.1016/j.anbehav.2004.03.013)
- Jawor, J. M. & Breitwisch, R. 2003 Melanin ornaments, honesty, and sexual selection. *Auk* **120**, 249–265. (doi:10.1642/0004-8038(2003)120[0249:MOHASS]2.0.CO;2)
- Kemp, D. J. 2002 Shedding new light on nature's brightest signals. *Trends Ecol. Evol.* **17**, 298–300. (doi:10.1016/S0169-5347(02)02516-8)
- Kolyer, J. M. & Reimschuessel, A. 1970 Scanning electron microscopy on wing scales of *Colias eurytheme*. *J. Res. Lepidoptera* **8**, 1–15.
- Makino, K., Satoh, K., Koike, M. & Ueno, N. 1952 Sex in *Pieris rapae* L. and the pteridine content of their wings. *Nature* **170**, 933–934. (doi:10.1038/170933a0)
- McGraw, K. J. & Hill, G. E. 2000 Differential effects of endoparasitism on the expression of carotenoid- and melanin-based ornamental coloration. *Proc. R. Soc. B* **267**, 1525–1531. (doi:10.1098/rspb.2000.1174)
- Meyer-Rochow, V. B. & Järvillehto, M. 1997 Ultraviolet colours in *Pieris napi* from Northern and Southern Finland: Arctic females are the brightest! *Naturwissenschaften* **84**, 165–168. (doi:10.1007/s001140050373)
- Obara, Y. 1970 Studies on the mating behavior of the white cabbage butterfly *Pieris rapae crucivora* Boisduval. III. Near-ultra-violet reflection as the signal of intraspecific communication. *Z. Vergl. Physiol.* **69**, 99–116. (doi:10.1007/BF00340912)
- Obara, Y. & Hidaka, T. 1968 Recognition of the female by the male, on the basis of ultra-violet reflection in the white cabbage butterfly, *Pieris rapae crucivora* Boisduval. *Proc. Jpn. Acad.* **44**, 829–832.
- Obara, Y. & Majerus, M. E. N. 2000 Initial mate recognition in the British cabbage butterfly, *Pieris rapae rapae*. *Zool. Sci.* **17**, 725–730. (doi:10.2108/zsj.17.725)
- Prum, R. O. & Torres, R. 2003 Structural colouration of avian skin: convergent evolution of coherently scattering dermal collagen arrays. *J. Exp. Biol.* **206**, 2409–2429. (doi:10.1242/jeb.00431)
- Rutowski, R. L. 1981 Sexual discrimination using visual cues in the checkered white butterfly (*Pieris protodice*). *Z. Tierpsychol.* **55**, 325–334.
- Rutowski, R. L., Macedonia, J. M., Morehouse, N. I. & Taylor-Taft, L. 2005 Pterin pigments amplify iridescent ultraviolet signal in males of the orange sulphur butterfly, *Colias eurytheme*. *Proc. R. Soc. B* **272**, 2329–2335. (doi:10.1098/rspb.2005.3216)
- Shawkey, M. D. & Hill, G. E. 2005 Carotenoids need structural colours to shine. *Biol. Lett.* **1**, 121–124. (doi:10.1098/rsbl.2004.0289)
- Stavenga, D. G., Stowe, S., Siebke, K., Zeil, J. & Arikawa, K. 2004 Butterfly wing colours: scale beads make white pierid wings brighter. *Proc. R. Soc. B* **271**, 1577–1584. (doi:10.1098/rspb.2004.2781)
- Stavenga, D. G., Giraldo, M. A. & Hoenders, B. J. 2006 Reflectance and transmittance of light scattering scales stacked on the wings of pierid butterflies. *Opt. Express* **14**, 4880–4890. (doi:10.1364/OE.14.004880)
- Vukusic, P., Sambles, J. R., Lawrence, C. R. & Wootton, R. J. 1999 Quantified interference and diffraction in single *Morpho* butterfly scales. *Proc. R. Soc. B* **266**, 1403–1411. (doi:10.1098/rspb.1999.0794)
- Vukusic, P., Sambles, J. R. & Ghiradella, H. 2000 Optical classification of microstructures in butterfly wing-scales. *Photon. Sci. News* **6**, 61–66.
- Vukusic, P., Sambles, J. R., Lawrence, C. R. & Wootton, R. J. 2001a Structural colour: now you see it—now you don't. *Nature* **410**, 36. (doi:10.1038/35065161)
- Vukusic, P., Sambles, R., Lawrence, C. & Wakely, G. 2001b Sculpted-multilayer optical effects in two species of *Papilio* butterfly. *Appl. Opt.* **40**, 1116–1125.
- Vukusic, P., Sambles, J. R. & Lawrence, C. R. 2004 Structurally assisted blackness in butterfly scales. *Proc. R. Soc. B* **271** (Suppl. 4), S237–S239. (doi:10.1098/rsbl.2003.0150)
- Waku, Y. & Kitagawa, M. 1986 Developmental process of scale pigment granules in the cabbage butterfly, *Pieris rapae crucivora*. *Jpn. J. Appl. Entomol. Z.* **30**, 35–42.
- Watt, W. B. 1964 Pteridine components of wing pigmentation in the butterfly *Colias eurytheme*. *Nature* **201**, 1326–1327. (doi:10.1038/2011326b0)
- Watt, W. B. & Bowden, S. R. 1966 Chemical phenotypes of pteridine colour forms in *Pieris* butterflies. *Nature* **210**, 304–306. (doi:10.1038/210304a0)
- Yagi, N. 1954 Note of electron microscopic research in pterin pigments in the scales of Pierid butterflies. *Annot. Zool. Jpn* **27**, 113–114.
- Yoshioka, S. & Kinoshita, S. 2006 Structural or pigmentary? Origin of the distinctive white stripe on the blue wing of a *Morpho* butterfly. *Proc. R. Soc. B* **273**, 129–134. (doi:10.1098/rspb.2005.3314)